

0.45 W diffraction-limited beam and single-frequency operation from antiguided phase-locked laser array with distributed feedback grating

M. P. Nesnidal, T. Earles, L. J. Mawst, and D. Botez^{a)}

Reed Center for Photonics, Electrical and Computer Engineering Department, University of Wisconsin-Madison, Madison, Wisconsin 53706

J. Buus

Gayton Photonics, Ltd., 6 Baker Street, Gayton, Northants NN7 3EZ, England

(Received 26 March 1998; accepted for publication 30 May 1998)

A second-order diffraction grating placed below the active region of a phase-locked resonant antiguided array selects the in-phase array mode in addition to its role as a single-longitudinal-mode selector. This type of array-mode discrimination relies on the fact that the resonant in-phase array mode has significantly better field overlap with the grating region than nonresonant array modes. Furthermore, it eliminates the need for a conventional array-mode discriminator: interelement loss; which can cause self-pulsations. Diffraction-limited beam and single-frequency operation is obtained to at least 0.45 W peak pulsed power from 20 element, InGaAs/InGaP/GaAs structures ($\lambda = 0.97 \mu\text{m}$) of 120- μm -wide aperture. Distributed-feedback operation is confirmed over the 20–40 °C temperature range. The results are in good agreement with theory. © 1998 American Institute of Physics. [S0003-6951(98)02531-5]

The ability to produce high-power, single-frequency, single-spatial-mode light sources is of fundamental importance to applications such as coherent free-space optical communications, blue-light generation via frequency doubling, midinfrared light generation via parametric frequency conversion, and low-noise sources for high-fidelity rf optical links. Large-aperture ($\geq 100 \mu\text{m}$) devices such as the fanout-type master-oscillator power amplifier (MOPA)¹ and the α -distributed-feedback (DFB) laser² have displayed high diffraction-limited, single-frequency powers. However, such devices, having weak or no lateral-mode confinement, possess inherent instabilities,^{3–6} thus raising serious issues of long-term stability and reliability. Therefore, there is a need for coherent large-aperture devices which not only select fundamental-mode operation but also maintain a stable mode to high drive levels.

As in the case of single-element devices, large-aperture emitters can achieve lateral-mode stability only by introducing strong built-in index guiding ($\Delta n \geq 0.01$). Resonant antiguided diode laser arrays (ROW arrays)⁷ with 100–200- μm -wide apertures have demonstrated the ability to operate in-phase with stable, diffraction-limited or near-diffraction-limited beams to record-high pulsed and cw output powers.^{7–10} Such performances are due primarily to the devices' high effective-index step ($\Delta n_{\text{eff}} \sim 0.05$) and inherent stability against multimoding via gain spatial hole burning (GSHB).¹¹ Discrimination against higher order spatial modes is usually provided by placing loss in the high effective-index interelement regions,⁷ in turn suppressing modes with significant interelement field. However, it has been shown¹² that the presence of interelement loss could trigger self-pulsations due to saturable absorption at high power levels. Therefore, in order to assure stable, coherent high powers

from antiguided arrays, there is a need for a novel spatial-mode selector that does not rely on interelement loss.

Here we present the first experimental proof of the concept¹³ that a DFB grating placed below the active region of a ROW array selects both a single longitudinal mode as well as a single lateral mode. Specifically we obtain pure, stable single-mode operation to at least 0.45 W peak pulsed power from 20 element, 120- μm -aperture devices.

A schematic representation of the ROW-LDFB structure is shown in Fig. 1. The structure is Al free, thus allowing for easy regrowths over gratings¹⁴ for longitudinal-mode control, and over patterned structures⁹ for lateral-mode stabilization and control. All layers are grown by low-pressure metalorganic chemical vapor deposition (LP-MOCVD) at around 700 °C. After growing a 0.5- μm -thick *n*-InGaP cladding layer on the GaAs substrate, a second-order sinusoidal DFB grating, with a tooth height of 75 and 300 nm period, is made by holographic interference and wet chemical etching. A GaAs “grating” layer is then formed by regrowth. The rest of the regrowth consists of a 325-nm-thick *n*-InGaP spacer layer, a separate confinement heterostructure (SCH) incorporating 200-nm-thick InGaAsP ($E_g = 1.62 \text{ eV}$) optical confinement layers surrounding two 7-nm-thick In_{0.2}Ga_{0.8}As quantum wells, a 150-nm-thick *p*-InGaP spacer layer, and a 180-nm-thick GaAs layer. The high effective-index interelement (array) regions are then defined by wet chemical etching of the GaAs layer and regrowing *p*-InGaP [Fig. 1(b)]. As a result a lateral effective-index step of 0.026 is obtained between the interelement and element regions of the array. The second regrowth consists of a 1- μm -thick *p*-InGaP layer and a 0.2- μm -thick *p*⁺-GaAs cap layer. 20-element arrays of two different values for the element width, *d*: 4.0 and 4.5 μm ; were studied. In both cases the interelement width, *s*, is 1.5 μm , which corresponds to the resonance of the in-phase mode.⁷

The modal behavior for ROW arrays has been previ-

^{a)}Electronic mail: botez@engr.wisc.edu

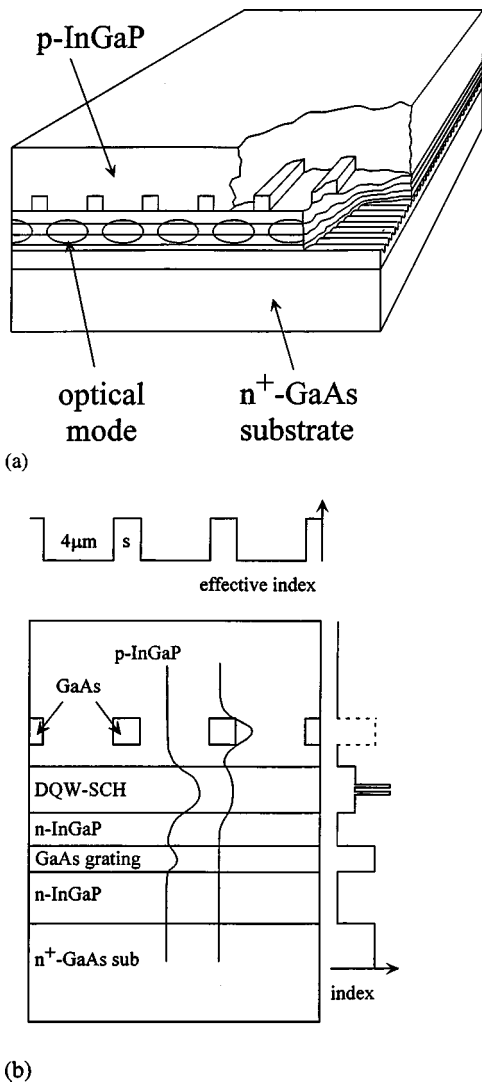


FIG. 1. Schematic representation of ROW-LDFB device: (a) 3D view; (b) cross-sectional view for an array of 4- μm -wide elements. A second-order DFB grating ($\Lambda = 300\text{ nm}$) is etched into the $n\text{-InGaP}$ cladding layer prior to the first regrowth.

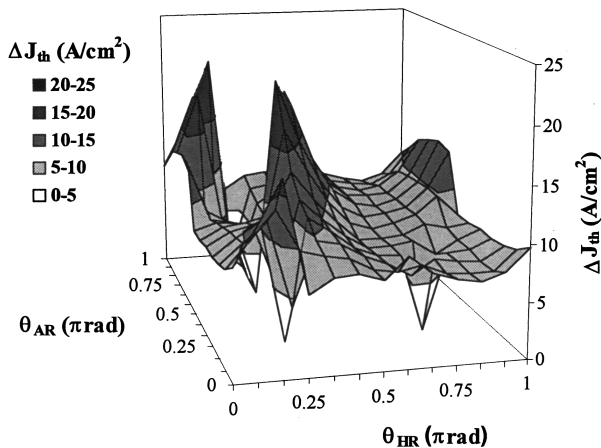


FIG. 2. Difference in threshold-current density, ΔJ_{th} , between the closest nonresonant mode and the in-phase resonant mode as a function of the grating phase with respect to the AR-coated and HR-coated facets; θ_{AR} and θ_{HR} , respectively. The array has 20 elements, 3%/95% facet-coating reflectivities, and is 350 μm long.

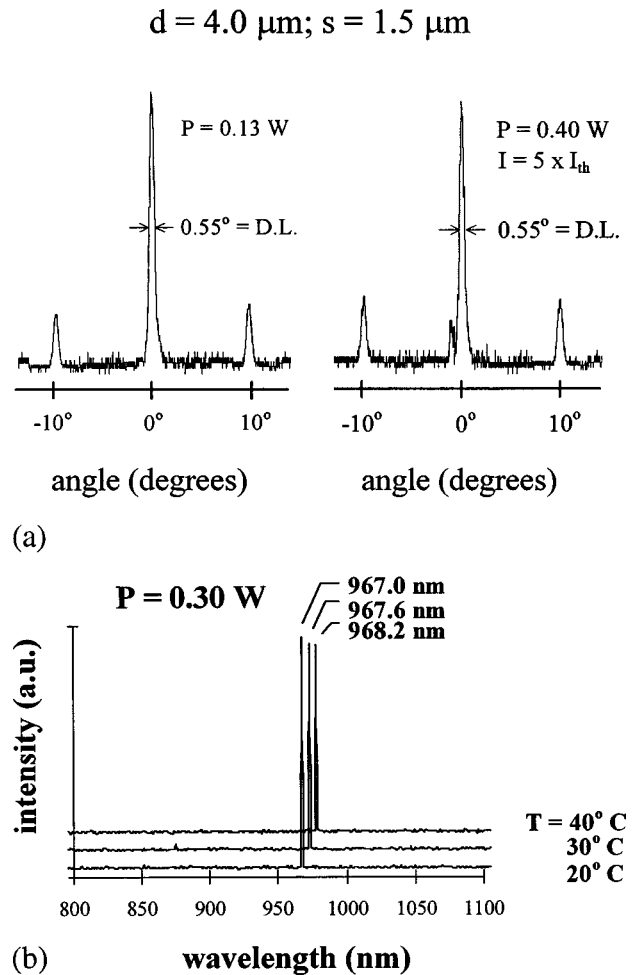


FIG. 3. Characteristics of 20-element, 3%/95%-coated 110- μm -aperture devices: (a) Diffraction-limited (DL) far-field beam patterns up to the 0.4 W power level. I_{th} is the threshold current; (b) spectra at 2 A (i.e., 0.3 W output) as a function of heat sink temperature.

ously discussed in detail.⁷ Array modes (i.e., spatial modes) are named according to the number of intensity nulls. For 20-element arrays, in addition to the desired in-phase array mode 38, the competing spatial modes are the upper and lower out-of-phase modes 57 and 19, and the upper and lower adjacent modes 39 and 37. In the element regions the field in the transverse direction is mainly located in the SCH structure [see Fig. 1(b)], while in the interelement regions the field is located primarily in the high-index GaAs passive guides.

For DFB laser structures the grating is typically placed above the active region at the upper confinement interface for ease of regrowth and fabrication. For such configurations, however, both element and interelement fields would significantly overlap the grating interface. As a result, all array modes would couple nearly equally to the grating. However, when the grating is placed below the active region, as shown in Fig. 1(b), coupling of the interelement field is insignificant, and the percentage of optical feedback for a given array mode depends on the percentage of its field intensity in the element regions.¹³ Because only the resonant in-phase array mode has virtually all its field in the element regions,⁷ it follows [see Fig. 1(b)] that it couples strongest to the grating compared to the other array modes. Therefore, a DFB grating placed below the active region acts simultaneously as a

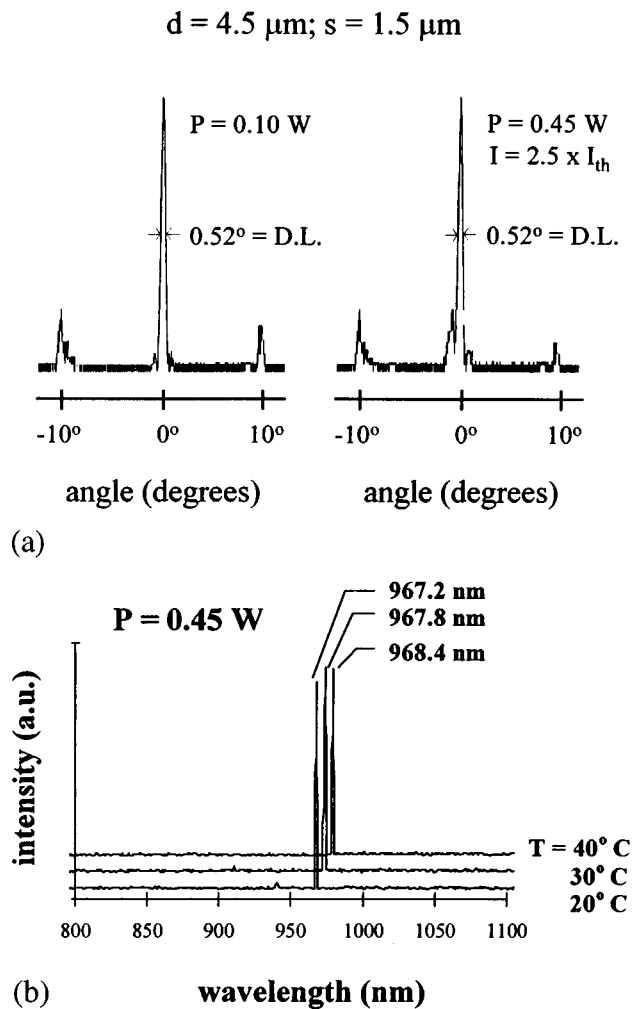


FIG. 4. Characteristic of 20-element, 3%/30%-coated 120- μm -aperture devices: (a) Diffraction-limited (DL), far-field beam patterns up to the 0.45 W power level; (b) spectra at 0.45 W output as a function of heat sink temperature.

single-frequency- and in-phase-mode selector.

The intermodal discrimination is shown in Fig. 2 for a 20-element ROW-LDFB array structure with 3%/95% anti-reflective (AR)/high-reflective (HR) coatings. The details of the calculation are presented elsewhere.¹³ The difference in threshold-current density, ΔJ_{th} , between the lower out-of-phase mode (i.e., mode 19) and the in-phase resonant mode (i.e., mode 38) is plotted as a function of the grating phases: θ_{AR} and θ_{HR} ; at AR-coated and HR-coated cleaved facets, respectively. (J_{th} lies in the 325–475 A/cm² range.) In-phase-mode operation is favored for all cleave locations. Single-longitudinal-mode operation occurs virtually everywhere, the exceptions being three degeneracy points at: $(\theta_{\text{AR}}, \theta_{\text{HR}}) = (\pi/4, \pi/4)$, $(\pi/4, 3\pi/4)$, and $(3\pi/4, \pi/4)$; where in-phase-mode operation is obtained in two longitudinal modes. The maximum discrimination, ΔJ_{th} , is 21 A/cm². Even though the amount of intermodal discrimination is relatively small, single spatial-mode operation is assured to high powers due to the immunity of the resonant in-phase mode to multimoding via GSHB.¹¹ More specifically, since the resonant in-phase mode has a uniform near-field intensity profile it uses all available gain, preventing other array modes from lasing at high drive levels.¹¹

Preliminary experimental results under pulsed operation

(5- μs -wide pulses, 2 kHz repetition rate) from 20-element ROW-LDFB devices are shown in Figs. 3 and 4. In Fig. 3 we show the beam patterns and spectra from a 500- μm -long device with 3%/95% facet coatings. The device emits in a diffraction-limited (0.55°) beam pattern [Fig. 3(a)] from a 110- μm -wide aperture, to 0.4 W peak power and $5\times$ threshold at 2.5 A drive current. Single-frequency operation is recorded to 0.4 W as well. Figure 3(b) displays the spectrum at a 2 A drive current as a function of heatsink temperature. The temperature dependence is $0.6 \text{ \AA}/^\circ\text{C}$, confirming DFB behavior. The fact that only one longitudinal mode lases is validated by the fact that the longitudinal-mode spacing (i.e., 2.2 \AA from theory and subthreshold spectra) is significantly larger than the spectrometer-limited spectral width ($\sim 1 \text{ \AA}$). In Fig. 4 we show the beam patterns and spectra from a 750- μm -long device with 3%/30% facet reflectivities. 0.45 W diffraction-limited power is obtained, with 75% central-lobe energy content [Fig. 4(a)]. At the 0.45 W power level single-mode DFB action is confirmed over the 20–40 $^\circ\text{C}$ temperature range [Fig. 4(b)].

These preliminary results confirm that the lower DFB grating selects both a longitudinal mode as well as a stable, lateral mode. Various optimizations (e.g., adjusting the device grating coupling for maximum output power in a single longitudinal mode)¹⁴ should allow for cw operation in a stable, diffraction-limited beam to watt-range powers.

In conclusion, we present the first demonstration of a phase-locked array for which a DFB grating acts as an array-mode selector. Single-frequency and single-spatial-mode operation are achieved to 0.45 W peak power from unoptimized devices. Therefore, ROW-LDBF arrays have the potential for stable beam, reliable operation to watt-range coherent powers.

This work was supported by NSF under Grant No. ECS-9522035.

¹D. F. Welch and D. G. Mehuys, *Diode Laser Arrays*, edited by D. Botez and D. R. Scifres (Cambridge University Press, Cambridge, UK, 1994), pp. 72–122.

²K. M. Dzurko, R. J. Lang, D. F. Welch, D. R. Scifres, and A. Hardy, Proc. IEEE/LEOS 1995 Annual Mtg. **2**, 400 (1995).

³L. Goldberg, M. Surette, and D. Mehuys, Appl. Phys. Lett. **62**, 2304 (1993).

⁴A. Schoenfelder, S. D. DeMars, K. M. Dzurko, R. J. Lang, D. F. Welch, D. R. Scifres, and A. Hardy, Tech. Dig. 15th IEEE International Semiconductor Laser Conference, Haifa, Israel, Paper PDP7, October 1996.

⁵D. J. Bossert, G. C. Dente, and M. L. Tilton, Proc. SPIE **3001**, 63 (1997).

⁶A. Egan, C. Z. Ning, J. V. Moloney, R. A. Indik, M. W. Wright, D. J. Bossert, and J. G. McInerney, IEEE J. Quantum Electron. **34**, 166 (1998).

⁷D. Botez, *Diode Laser Arrays*, edited by D. Botez and D. R. Scifres (Cambridge University Press, Cambridge, UK, 1994), pp. 1–71.

⁸J. M. Gray, J. H. Marsh, and J. S. Roberts, IEEE Photonics Technol. Lett. **10**, 328 (1998).

⁹H. Yang, L. J. Mawst, M. Nesnidal, J. Lopez, A. Bhattacharya, and D. Botez, Electron. Lett. **33**, 136 (1997).

¹⁰J. S. O, P. S. Zory, C. F. Miester, J. Yoon, M. A. Emanuel, V. R. Sperry, B. D. Schwartz, and R. Setzko, Proc. SPIE **3284**, 36 (1998).

¹¹R. F. Nabiev and D. Botez, IEEE J. Sel. Top. Quantum Electron. **1**, 138 (1995).

¹²S. Ramanujan, H. G. Winful, M. Felisky, R. K. DeFreez, D. Botez, M. Jansen, and P. Wiseman, Appl. Phys. Lett. **64**, 827 (1994).

¹³M. P. Nesnidal, L. J. Mawst, D. Botez, and J. Buus, IEEE Photonics Technol. Lett. **10**, 507 (1998).

¹⁴T. Earles, L. J. Mawst, and D. Botez, Tech. Dig. IEEE/OSA Conf. Lasers Electro-Optics'98, San Francisco, CA, **6**, 38 (1998).